JOURNAL OF MATERIALS SCIENCE 21 (1986) 4456–4462

A TEM study of ordering in the perovskite, $Pb(Sc_{1/2}Ta_{1/2})O_3$

C. A. RANDALL, D. J. BARBER
Department of Physics, University of Essex, Colchester CO4 3SQ, UK
R. W. WHATMORE
Allen Clark Research Centre, Towcester NN12 8EQ, UK
P. GROVES
Clarendon Laboratory, Oxford OX1 3PU, UK

Ordering behaviour and the factors which influence the ordering have been studied in both single crystals and hot-pressed ceramics of $Pb(Sc_{1/2}Ta_{1/2})O_3$ using TEM techniques, including low-temperature microscopy. The characteristics of the structurally-ordered domains are described and also the observation by electron diffraction of new superlattice reflections and diffuse scattering in both the paraelectric and ferroelectric phases. The superlattice reflections are interpreted in terms of Pb^{2+} cation displacements. The non-interaction of ordered domains and ferroelectric domains is explained within this model.

1. Introduction

Oxides with the perovskite structure, corresponding to the general formula ABO_3, have B ions at the centres of regular octahedra of oxygen ions and A ions occupying holes between the octahedra [1, 2]. $Pb(Sc_{1/2}Ta_{1/2})O_3$, usually abbreviated to PST, has the lead ion on the A-site whereas the B-site can be occupied by either scandium or tantalum. Upon isothermal annealing at high temperatures, the B-site cations, Sc^{3+} and Ta^{5+}, tend to order themselves. The dielectric properties of PST are seen to be dependent on the degree of order [3, 4]. For example, the transition temperature can be adjusted by changing the degree of order: for fully disordered PST the transition temperature is $\sim 0°$ C while for ordered PST it is $\sim 26°$ C. At the transition temperature the crystal structure changes from a cubic symmetry to a rhombohedral symmetry with rhombohedral lattice parameter ~ 0.4072 nm [5, 6]. The first TEM study of PST was carried out by Harmer *et al.* [7], who characterized the antiphase boundaries (APBs) of the ordered domains. Chang and Chen [8] have recently published the results of an investigation of PST at liquid nitrogen temperatures and found no strong interactions between APBs and ferroelectric domains.

2. Experimental details

The single crystals were grown from a PbF_2–PbO–B_2O_3 flux as described by Setter and Cross [9] and the ceramics were prepared by hot-pressing methods. The ceramics had a grain size of 5 μm. Annealing of the single crystals was carried out for various times at temperatures of $\sim 700°$ C, both in air and in a crucible packed with $PbZrO_3$. Subsequently samples were cut from the annealed specimens and polished down to a thickness of $\sim 30\,\mu$m prior to ion-beam thinning at 5 kV, thereby enabling observations to be made by transmission electron microscopy (TEM). The TEM analysis was performed on a JEOL-200CX with Link Systems energy-dispersive X-ray analysis equipment, including a high take-off angle spectrometer (EDS). Cold-stage experiments were performed at Imperial College, London using an AEI-EM7 electron microscope which was operated at 300 kV.

3. Results

3.1. The nucleation of structurally-ordered domains in single-crystal PST

A number of PST single crystals were taken and annealed for various lengths of time to allow the kinetics of the ordering process to be investigated. The unannealed as-grown samples have very weak F-type (ordering) electron diffraction spots. These spots are the result of the scandium and tantalum cations occupying alternating B-sites (i.e. ordering on them). This produces a superlattice doubling of the unit cells to $(2a_0 \times 2a_0 \times 2a_0)$ and results in a face-centring of the B-cations on the lattice (hence the designation "F-type" to the corresponding electron reflections). Using an F-reflection to give a dark-field (DF) image, as shown in Fig. 1a, small ordered domains are seen. The average size of the ordered domains was determined by a line intercept method. Fig. 1b shows the corresponding $\langle 1\,1\,0 \rangle$ zone axis selected-area diffraction pattern. In the as-grown crystals the average domain size was 2 mm. Figs 2 to 5 show the effect of the time of annealing on the size of the ordered domains. Not only does their size increase but so also does the intensity of the superlattice (F-type) reflections $\{h + 1/2,\ k + 1/2,\ l + 1/2\}$ as previously reported by Setter and Cross [3], who used X-ray powder diffraction techniques.

Our observations further indicate that the ordering process is not homogeneous within the crystals, there

0022–2461/86 $03.00 + .12

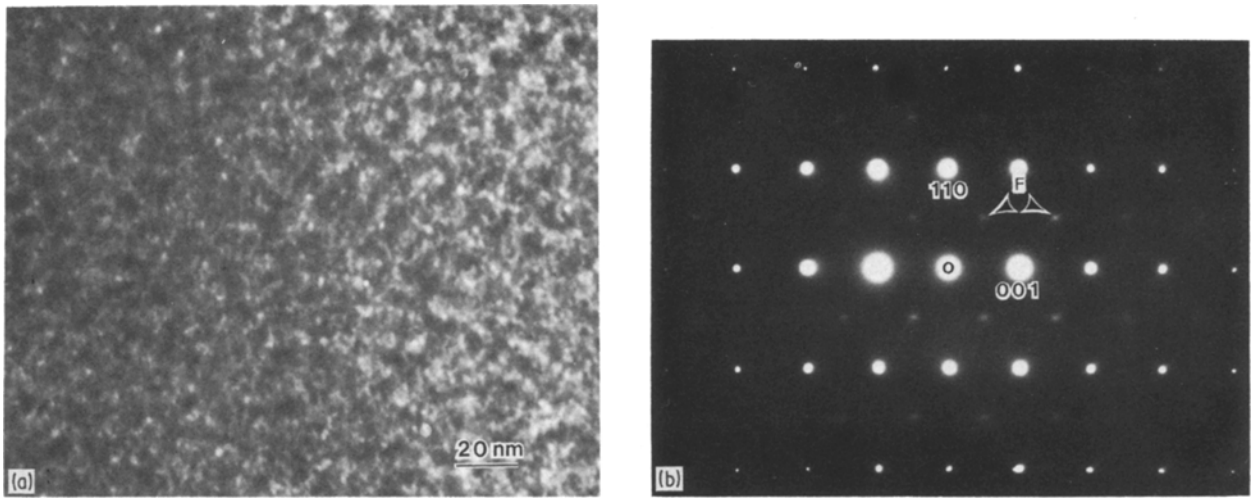

Figure 1 (a) DF image of unannealed sample of PST showing very small ordered domains, ~2 nm in size. (b) ⟨1 1 0⟩ zone-axis electron diffraction pattern from an unannealed PST crystal. Very weak F-type ordering spots are visible (arrowed).

being slight variations in domain size. The latter is probably influenced by non-uniformities in composition and stoichiometry. Any results obtained by X-ray methods are only an average of the whole crystal and therefore are not sensitive to the slight chemical variations that can exist throughout the crystal. However, an exceptional case was found by TEM in one of the crystals, where a sharp interface was observed between two regions with ordered domains of differing sizes, as shown in Fig. 6. Selected-area diffraction patterns taken from this region showed no elongation or splitting of the strong non-superlattice spots, indicating that there is little change in the lattice parameter between the two states of order. The magnitude of the domain diameter changed by approximately 100 times, being ~120 nm in the region with the small domains. Analysis by TEM/EDS showed that the large ordered domains are lead-rich, the rest of the crystal being slightly lead-deficient (presumably because of loss of PbO during annealing). The chemical composition of the region with the large domains was $\sim Pb_{1.02}(Sc_{0.49}Ta_{0.51})O_{3+\delta}$ and for the region with the smaller domains it was $\sim Pb_{0.98}(Sc_{0.49}Ta_{0.51})O_{3-\delta}$.

In general we find that the size of ordered domains obtained in PST single crystals with long annealing times is smaller than that obtained in PST ceramics with similar heat treatment, in agreement with Setter and Cross [3]. We therefore conclude that grain boundaries have an important influence on the ordering mechanism (in partially ordered grains the larger domains are found around the grain peripheries). In single crystals, sub-grain boundaries appear to have a similar effect on the ordered-domain microstructure. In highly ordered ceramics, the APBs are pinned by grain boundaries and other microstructural defects; this limits the complete ordering of a grain. Fig. 7a illustrates the pinning of APBs by high-angle boundaries and also by particles of second phase in highly ordered PST ceramic. Fig. 7b shows a grain in partially ordered PST that has larger ordered domains near the grain boundaries, but pinning is still apparent. No chemical inhomogeneities were detected within these grains. Both tilt and twist sub-grain boundaries are also pinning sites for APBs. Fig. 7c shows two 7° tilt sub-grain boundaries that pin ordered domains within a lead-rich region of a single crystal of PST.

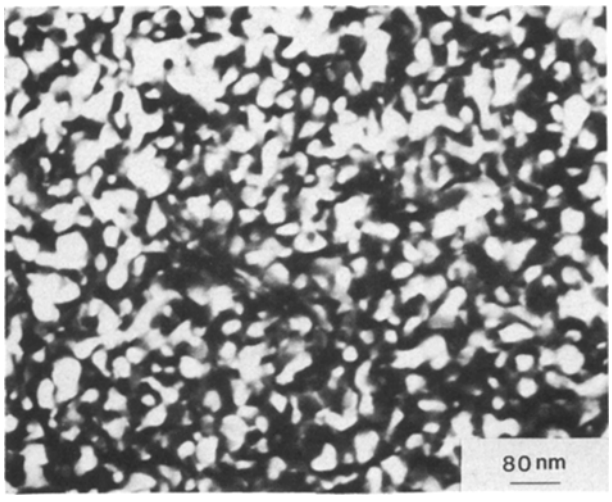

Figure 2 PST after annealing at 700° C for $2\frac{1}{2}$ h. The domains have grown to an average size of ~40 nm.

3.2. The ferroelectric phase and superlattice reflections in PST

Chang and Chen [8] reported that they did not see any $\{\frac{1}{2}\frac{1}{2}0\}$ type reflections from PST but we found that long exposures revealed weak $(\frac{1}{2}\frac{1}{2}0)$, $(\frac{3}{2}\frac{1}{2}0)$, etc. spots (denoted as α-spots) in partially-ordered ceramics and single crystals. Fig. 8a shows a ⟨0 0 1⟩ zone electron diffraction pattern of PST at room temperature. We also observed thermal diffuse scattering in ⟨1 1 0⟩ directions in reciprocal space, features which are similar to those found with modified PZT [10] and other lead-based perovskites. The cause of this diffuse scattering will be discussed in another paper.

When the temperature of a PST crystal is lowered to −150° C by means of a liquid nitrogen-cooled specimen stage, ferroelectric domains are induced. The α-type reflections are also enhanced in intensity and a new set of spots appear at reciprocal lattice positions $(\frac{1}{2}00)$, $(\frac{3}{2}00)$, etc. (denoted β-spots). These are

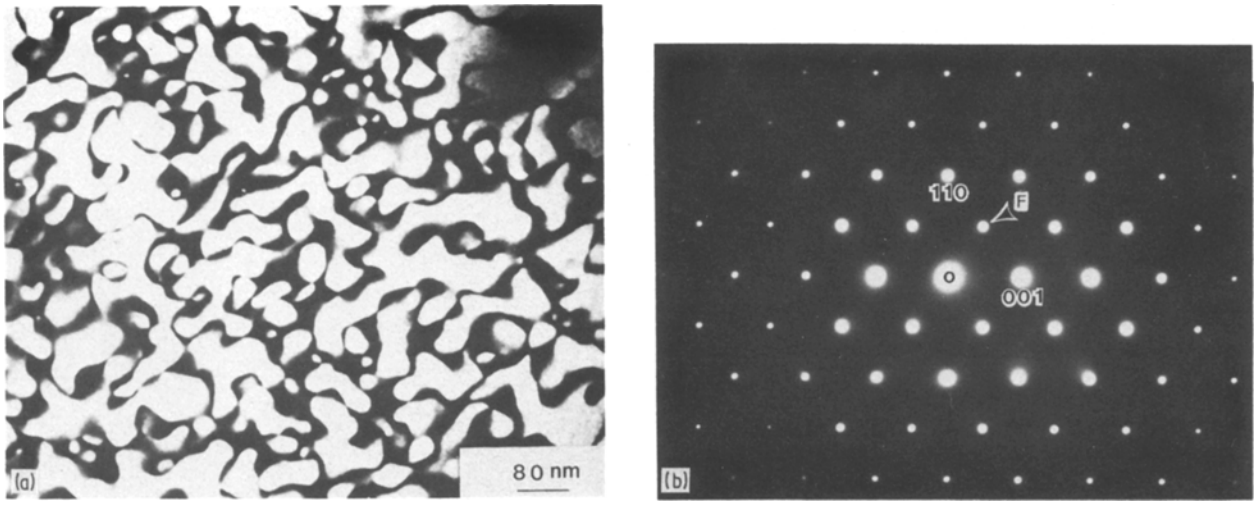

Figure 3 (a) PST after annealing at 700° C for 5 h. The ordered domains have grown to an average size of ~ 120 nm. (b) Electron diffraction pattern from PST which has been annealed at 700° C for 5 h.

illustrated in Figs 8b and c, which show ⟨0 0 1⟩ and ⟨1 1 0⟩ zone diffraction patterns, respectively. Fig. 9a, recorded with the single crystal specimen at − 150° C, shows the ferroelectric domains in PST: the dipole displacement is in a ⟨1 1 1⟩ direction in the rhombohedral phase and the low-energy domain walls are parallel to {1 1 0} planes, as apparent from the above micrograph. The presence of twin-like domains causes elongation and spot splitting on the selected-area diffraction patterns. No strong interaction between APBs and ferroelectric domains was found. By using the heat of the electron beam we could cause the domains to vanish and we could observe the positions where they nucleated on reappearing; Fig. 9b shows a typical result. We conclude that APBs are not generally either nucleation or pinning sites for the ferroelectric domains. We are therefore in agreement with Chang and Chen [8] that there is no strong interaction between APBs and ferroelectric domains.

3.3. Superlattice spots in relation to specimen temperature and the zone axis of the diffraction pattern

From ⟨1 1 0⟩ zone-axis diffraction patterns taken at room temperature and at − 150° C from single-crystal specimens (Figs 3b and 8c, respectively) it is apparent that the α- and β-superlattice spots are only present in the low-temperature study, and that the intensities of these two sets of spots are then similar. However, in ⟨0 0 1⟩ zone patterns the behaviour is rather different: at room temperatures the α-spots are present but not the β-spots (Fig. 8a), whereas at low temperatures (− 150° C) (where ferroelectric domains appear) both sets of spots are present but the α-set is significantly stronger (Fig. 8b). Even before the appearance of β-spots in the ⟨0 0 1⟩ zone patterns, there is a gradually strengthening of the α-spots. The α-spots are found in the diffraction patterns of other zones, for example ⟨1 1 1⟩ and ⟨1 2 1⟩. These α-spots are also found at temperatures well above the transition temperature — in fact, they have been observed at temperatures of ~ 350° C. The occurrences of α-reflections in the case of other lead-based perovskites, PLZT (lead–lanthanum zirconium titanate) and modified PZT at room temperature, have been confirmed using X-ray powder diffraction techniques.

At temperatures of about − 140° C, localized electron-beam heating was used to cause the disappearance of ferroelectric domains and superlattice spots. On reducing the beam intensity the domain

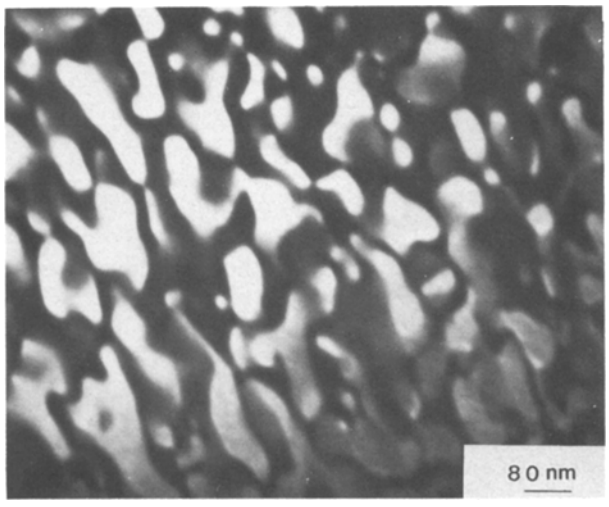

Figure 4 PST after annealing at 700° C for 8 h. The domains have grown to an average size of ~ 150 nm.

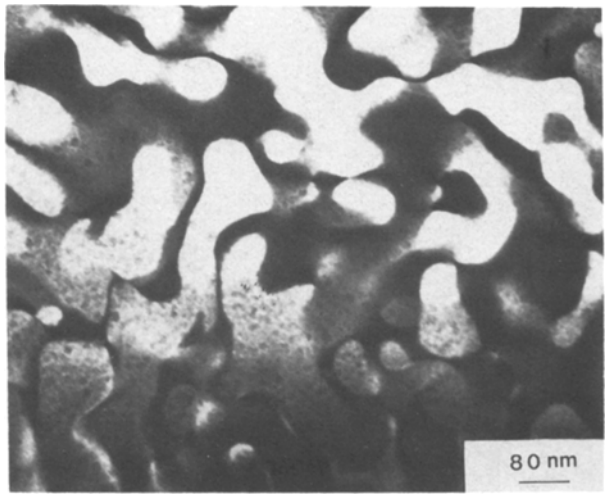

Figure 5 PST after annealing at 700° C for 16 h. The domain size is ~ 200 nm. There is evidence of PbO loss, in the form of a mottled background contrast.

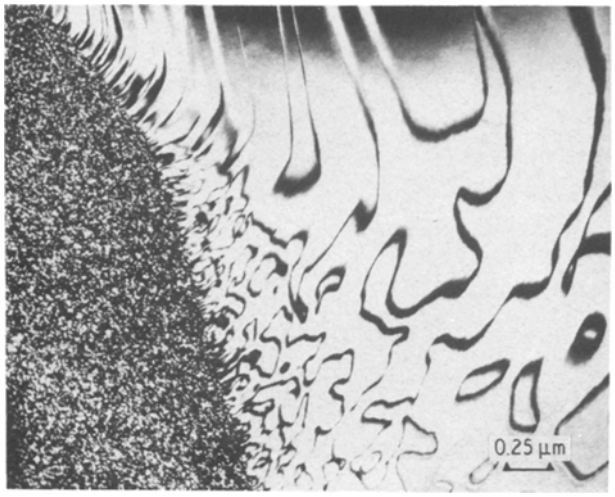

Figure 6 DF micrograph of an interface between two regions of differing domain size in a PST crystal. X-ray microanalysis by TEM/EDS reveals a change in lead concentration across the boundary.

contrast returns, together with the superlattice spots. In the ⟨0 0 1⟩ zone electron diffraction patterns the β-spots disappear but the α-spots remain. However, in the ⟨1 1 0⟩ zone pattern the disappearance of the domains is coupled with the disappearance of both the α- and β-spots. So, in summary, the presence of α-spots above the transition temperature and the dependence of α-spots upon the zone axis of the diffraction pattern have led us to believe that a two-fold explanation for α-spots is required, one dependent on the displacements of the Pb^{2+} ions (dipolar displacements) and the other independent of them, as discussed below.

4. Discussion

4.1. Dipole displacement model

Any equivalent (same magnitude and direction) displacements of all B-site cations in relation to the other lattice sites would only contribute to F-reflections and would not produce α- or β-diffraction spots. Any non-equivalent (either different magnitude and/or direction) displacements of the B-cations would weaken the F-reflection as the B-ordering site symmetry would no longer contribute. So the production of the additional spots could thus be associated with Pb^{2+} displacements. Recently, X-ray studies by Groves [6] on PST have let him to suggest that its displacive transition primarily involves displacements of Pb^{2+}. Such behaviour would be quite different from that of normal perovskites where B-site cations are displaced. The relative displacement of the lead cations in the low-temperature phase from their positions in the cubic paraelectric phase will induce an electric dipole between the lead cations and the oxygen anions. It will be interesting to see whether this effect occurs in other ordering, perovskite-structured oxides such as $Pb(Sc_{1/2}Nb_{1/2})O_3$ (abbreviation PSN).

The structure of the ferroelectric unit cell is based upon a pseudo-cubic $2a_0 \times 2a_0 \times 2a_0$ superlattice cell (where a_0 is the lattice parameter normal of the cubic perovskite cell), as shown in Fig. 10. Here B_1 and B_2 represent B-site cations in the F-type ordering positions. The $+\delta$ and $-\delta$ denote non-equivalent displacements of Pb^{2+} cations. We note here that our model ignores the scattering effects of the oxygen atoms, on the grounds that they are negligible compared to the scattering by cations.

The scattering factors for the first three superlattice

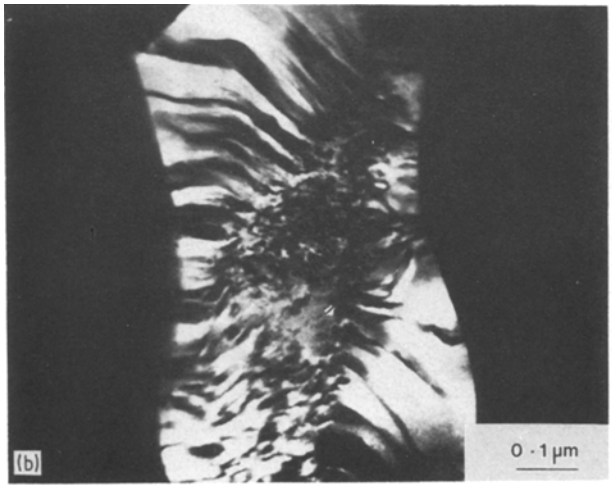

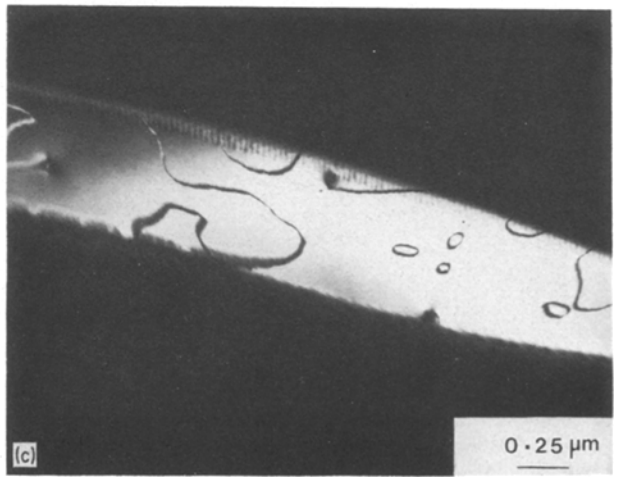

Figure 7 (a) DF micrograph of a grain in 80% ordered PST ceramic. The arrows indicate where domains are pinned at a grain boundary (A) and also pinning at a second-phase inclusion (B). (b) DF micrograph of a partially-ordered grain in hot-pressed PST showing a higher degree of ordering near the grain boundaries. (c) DF micrograph of single-crystal PST showing ordered domains which are pinned by two adjacent tilt boundaries corresponding to misorientations of about 7°.

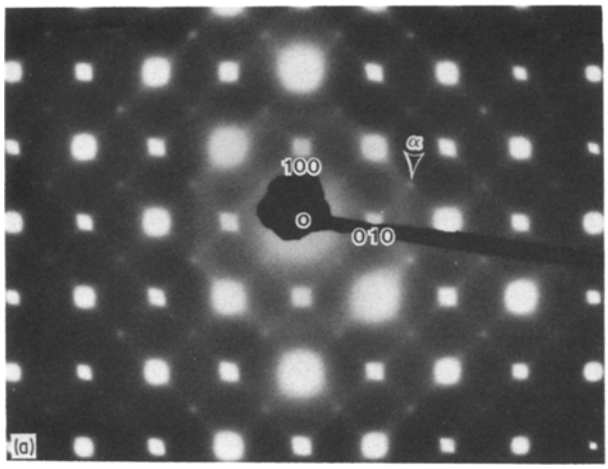

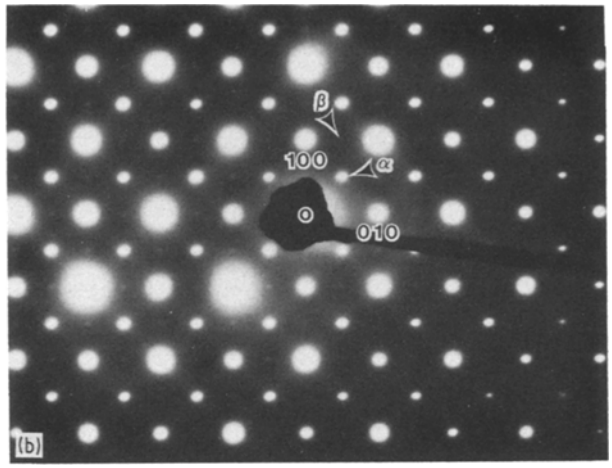

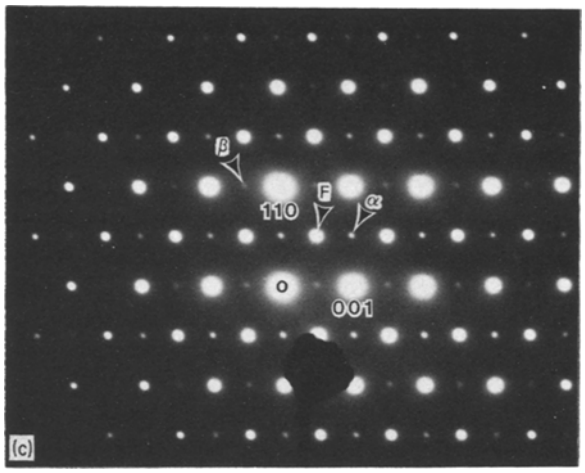

Figure 8 (a) ⟨0 0 1⟩ zone-axis electron diffraction pattern from PST at room temperature. Weak α-spots (arrowed) and diffuse scattering in ⟨1 1 0⟩ directions are visible. (Recorded at 300 kV). (b) ⟨0 0 1⟩ zone-axis electron diffraction pattern from PST at − 150° C. Superlattice spots, labelled α and β, are seen. Note the relative strengths of the α- and β-spots. (Recorded at 300 kV). (c) ⟨1 1 0⟩ zone-axis electron diffraction pattern from PST at − 150° C. F-type ordering spots, as well as α- and β-spots, are indicated. Note the similar intensities of the α- and β-spots. (Recorded at 300 kV).

spots are

$$F_{\frac{1}{2}00} = f_{Pb}(\cos 2\pi\delta^{+} - \cos 2\pi\delta^{-}) = f_{Pb+} - f_{Pb-}$$

$$F_{\frac{1}{2}\frac{1}{2}0} = f_{Pb+} - f_{Pb-}$$

$$F_{\frac{1}{2}\frac{1}{2}\frac{1}{2}} = f_{Pb+} - f_{Pb-} + 4(f_{B_1} - f_{B_2})$$

The last of these equations gives the enhanced intensity of the F-ordering spot.

The successes of this model are that it predicts the disappearance of spots of the α- and β-spots of comparable intensity in the ⟨1 1 0⟩ zone electron diffraction pattern and the disappearance of $\{\frac{1}{2}00\}$ type reflections in the ⟨0 0 1⟩ zone pattern. The scattering factors are directly dependent on the amount of distortion in the unit cell. In the ferroelectric phase the lead cation displacements gradually increase with the progressive lowering of the temperature. These displacements increase the difference in scattering factors and thus the intensity of the superlattice spots increases,

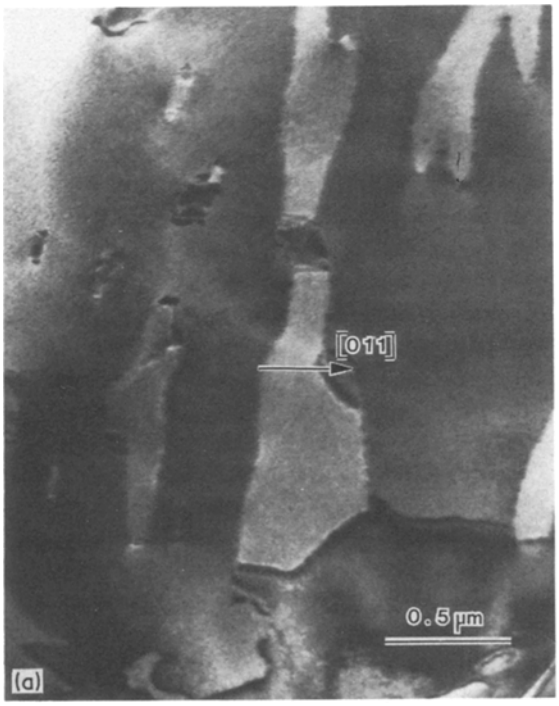

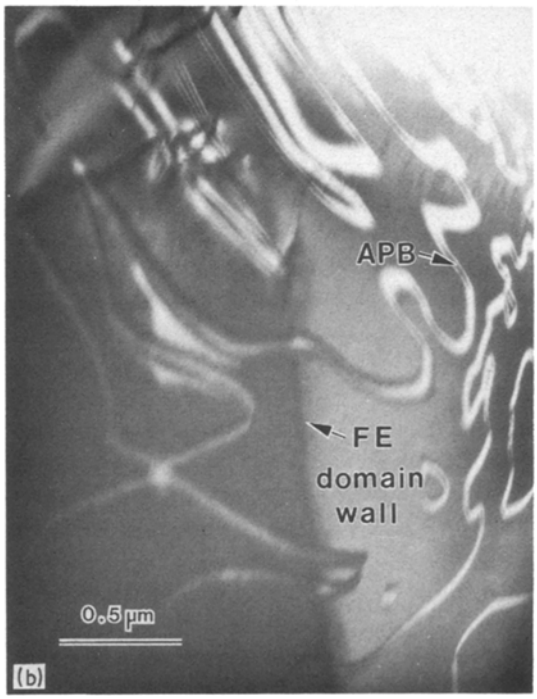

Figure 9 (a) BF micrograph illustrating ferroelectric domains in PST at − 150° C. (300 kV image obtained with EM7 microscope). (b) BF micrograph showing both ferroelectric domains and the APBs associated with structural order in PST at − 150° C. (300 kV image obtained with EM7 microscope).

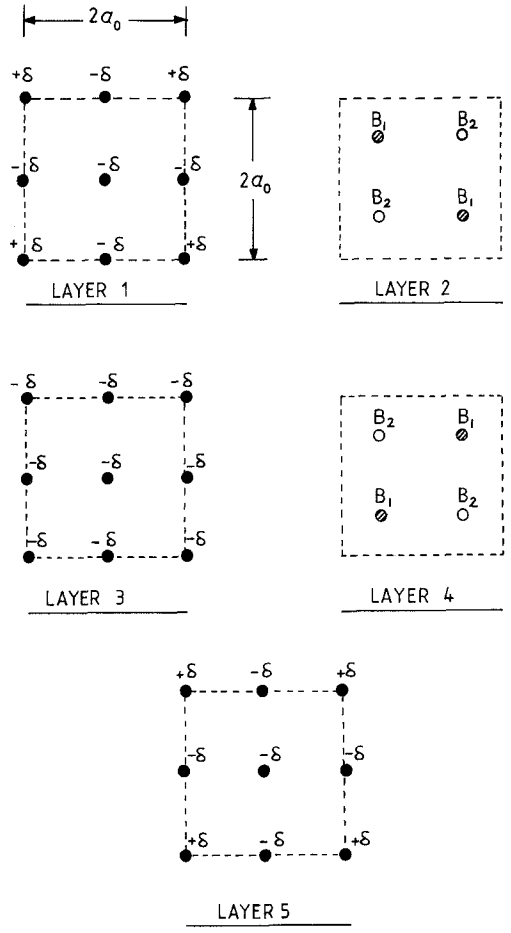

Figure 10 Diagram to show the arrangement and displacements of ions in relation to the dipole displacement model; (●) Pb^{2+} cation; (○) B_1-site atom (scandium, say); (○) B_2-site atom (tantalum, say); ($\pm\delta$) displacement of Pb^{2+} cation, the sign distinguishing between different displacements.

and these are eventually visible in the electron diffraction patterns. In the paraelectric phase there are no displacements of the lead cations (δ^+ and δ^- are both zero) and there is no difference between the scattering factors. Then

$$F_{\frac{1}{2}00} = 0$$

$$F_{\frac{1}{2}\frac{1}{2}0} = 0$$

$$F_{\frac{1}{2}\frac{1}{2}\frac{1}{2}} = 4\,(f_{B_1} - f_{B_2})$$

Because of the increased distortions in the ferroelectric phase on cooling, there is also an increase in the elastic strain energy and this is accommodated by the formation of ferroelectric domains. Ferroelectric domains have a twin-like relationship, as first shown by Tanaka and Honjo [11] for $BaTiO_3$ and by Randall *et al.* [10] for rhombohedral ferroelectrics. This results in the elongation and splitting of spots in the selected-area diffraction patterns.

The dipole displacement model does not, however, explain a number of observations such as the presence of the α-spots at high temperatures, and why these spots are stronger in the ⟨1 0 0⟩ zones. It is interesting that α-spots observed at room temperature are always found in the zones that exhibit diffuse scattering. No diffuse scattering is found in ⟨1 1 0⟩ zones and these have no α-spots at room temperature. We are continuing to develop a more complete model for the superlattice spots and the diffuse scattering, which seem to be associated with each other in lead-based perovskites.

4.2. Ordering behaviour

The ordering of a perovskite like PST or PSN affects the electrical properties and allows the possibility of manipulating the electrical properties to suit the application. The two main factors which control the degree of order on the B-sites of the perovskite structure are the electrostatic energy (ionic valence) and the elastic energy (ionic size).

Our observations show that the unannealed crystals have very small domains, ~2 nm in diameter. Ordering of the scandium and tantalum atoms between the B-sites, made possible by heat treatment, allows the electrostatic and elastic energies to be reduced and this is reflected in the strengthening of the F-type superlattice spots and the growth of the ordered domains. With long annealing times, structurally-ordered domains in single crystals can grow up to and beyond 200 nm in size. In the case of lead-based perovskites, samples used in long annealing experiments can suffer from PbO deficiency and so we restricted ourselves to no greater than 2% weight loss, which limits the possibility of growing very large domains. However, interactions between APBs and grain boundaries in the ceramics are complex. Regions adjacent to grain and sub-grain boundaries are known to have high vacancy concentrations (e.g. Atkinson and Taylor [12], Koschek and Kubalek [13]). So, in the early stages of hot pressing, we might expect the ordering process on the B-sites to be assisted by an enhanced vacancy concentration near the grain boundaries. In the later stages of hot pressing, grain boundaries inhibit ordering by pinning APBs.

An APB is a wall between two parts of the crystal across which the ordered atom sequences are out of phase: it is therefore a region of local disorder. Fig. 11 illustrates the situation which we assume to occur in PST. The smaller is the average diameter of ordered domains the greater the density of APBs, and thus the larger the degree of disorder.

Using this model we must conclude that 100% ordering implies that there will be no APBs in a grain or crystal. Such an ideal system is inhibited by the pinning of the APBs by other microstructural interfaces, second-phase particles, etc. It follows that in fine-grained ceramics it will be especially difficult to

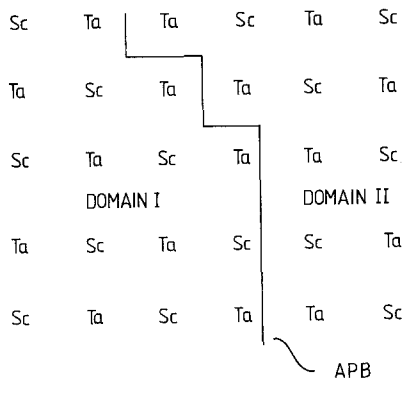

Figure 11 Two-dimensional representation of an APB in PST.

obtain a high degree of order because of these mechanisms. From our observations that a chemical interface affects the ordering in a single crystal (Fig. 5), we would expect regions of compositional inhomogeneity to exhibit variations in transition temperature.

An important success of the dipole displacement model is that because the ferroelectric domains are associated mainly with the Pb^{2+} cation displacements and the APBs are associated with the B-cation sublattice, we have an explanation of why no strong direct interaction is observed between these two types of "dynamic" microstructure, as noted by Chang and Chen [8] and in this study. Some caution must be used here, since the observations only pertain to thin films and in such films the elastic strain fields of some defects may be relaxed. Stronger interactions between the two forms of microstructure may occur in bulk materials.

5. Summary and conclusions

This TEM study shows that the ordering behaviour of the B-site cations in PST is influenced by (i) compositional inhomogeneity and (ii) defect microstructure, especially grain and sub-grain boundaries. Electron diffraction patterns obtained at room temperature and $-150^{\circ}C$ show significant differences: (iii) the presence of additional spots and (iv) elongation and splitting of spots owing to the presence of twin-like ferroelectric domains. These diffraction observations are explained in terms of non-equivalent displacements of adjacent A-site Pb^{2+} ions. A model which we offer is based upon and extends the ideas recently proposed by Groves [6] to explain X-ray data for PST. Phenomena which are specifically associated with the A-sites and B-sites (electric dipoles and structural ordering, respectively) appear to have no direct, strong interaction, as also noted experimentally by Chang and Chen [8].

Acknowledgements

The work was made possible through research grant GR/C/29072 and a CASE studentship (C.A.R.) sponsored by the Allen Clark Research Centre (Caswell), both awarded by the Science and Engineering Research Council (SERC). One of us (P.G.) also wishes to thank SERC for a research fellowship. We gratefully acknowledge access to the 1 MV AEI-EM7 electron microscope at the Imperial College of Science and Technology, London, and the assistance of Mr J. Woodall of Imperial College. We also thank Mr T. G. Goodwin of the University of Essex for his valuable technical assistance.

References

1. M. E. LINES and M. A. GLASS, "Principles and Applications of Ferroelectrics and Related Materials" (Clarendon Press, Oxford, 1977) p. 241.
2. H. A. MEGAW, "Crystal Structure: A Working Approach" (Saunders, Philadelphia, 1975) p. 217.
3. N. SETTER and L. E. CROSS, *J. Appl. Phys.* **51** (1980) 8.
4. C. C. F. STENGER and A. J. BURGRAAF, *Phys. Status Solidi (a)* **61** (1980) 275.
5. N. SETTER and L. E. CROSS, *Ferroelectrics* **37** (1981) 551.
6. P. GROVES, *J. Phys. C: Solid State Phys.* **18** (1985) L1073.
7. M. HARMER, A. BHALLA, B. FOX and L. E. CROSS, *Mater. Lett.* **2** (4A) (1984) 278.
8. Y. CHANG and Z. CHEN, *Ferroelectr. Lett.* **4** (1985) 13.
9. N. SETTER and L. E. CROSS, *J. Cryst. Growth* **50** (1980) 555.
10. C. A. RANDALL, D. J. BARBER and R. W. WHATMORE, in Proceedings of EMAG '85, Newcastle-upon-Tyne, Conference Series No. 78 (Institute of Physics, London, 1985) p. 53).
11. M. TANAKA and G. HONJO, *J. Phys. Soc. Jpn* **19** (1964) 954.
12. A. ATKINSON and R. I. TAYLOR, *Phil. Mag.* **A43** (1981) 979.
13. G. KOSCHEK and E. KUBALEK, *J. Amer. Ceram. Soc.* **68** (1985) 582.

Received 11 February
and accepted 28 April 1986